suggests that doped anions may play a major role in order to decide if the PPy film is conductive.

There are still a few unknown factors that might contribute to the observed conductivity of the PPy–CuPcTs thin-film electrode when the PPy is in a neutral form. The role of cations, such as MV^{2+} and Na^+, for the conductive nature of the film is not known at this stage. Also unknown is the behavior of the PPy-O during the reduction reaction of the PPy–CuPcTs film, but it is quite unlikely that the PPy-O would play the major role for the conductive nature of the PPy–CuPcTs electrode. Although the high oxygen content in the PPy film doped with inorganic anions has been reported,[28] this type of PPy film behaves as an insulator when it is reduced.

Acknowledgment. This work was supported in part by the Office of Naval Research (Grant N00014-89-J-1339) and the National Institutes of Health (Grant SO6G08047).

(28) Bi, X.; Yao, Y.; Wan, M.; Wang, P.; Xiao, K.; Yang, Q.; Qian, R. *Makromol. Chem.* **1985**, *186*, 1101.

Stereochemistry and Curvature Effects in Supramolecular Organization and Separation Processes of Micellar *N*-Alkylaldonamide Mixtures

Jürgen-Hinrich Fuhrhop* and Christoph Boettcher

Contribution from the Institut für Organische Chemie der Freien Universität Berlin, Takustrasse 3, D-1000 Berlin 33, West Germany. *Received June 21, 1989*

Abstract: D- or L-configured glucon-, mannon-, and galactonamides bearing *N*-octyl or *N*-dodecyl substituents were mixed pairwise in a 1:1 molar ratio in aqueous solution and then converted to micellar fibers. By electron microscopy we observed chain length induced racemate resolution, formation of simple or complex hybrid structures or quantitative separation of individual fibers, as well as ideal mixing of the components within one fiber. Separations were traced back to stereochemical dissimilarities between the outer hydroxymethine groups of both components. Different lengths of the hydrophobic chains slowed fiber formation down and allowed the detection of intermediate micellar clusters.

Hydrophobic bilayers are soft materials and capable of being shaped by stereoselective interactions of chiral head groups as well as by strong hydrogen bonds between secondary amide groups. Helical tubes and rods and twisted ribbons and rolled-up sheets have thus been obtained in aqueous gels by self-organization of appropriate spherical or sheet-like bilayers made of lipid molecules.[1-3] This paper describes for the first time the formation of mixed aggregates ("alloys") as well as of bistructural and of fully separated fiber aggregates. Evidence for separations or nonseparations comes from comparison of electron micrographs of the mixtures with those of the individual components and, in one case, from electron micrographs of autoradiographs.

As a starting point we chose the amphiphilic *N*-alkylaldonamides with D- or L- gluon, mannon, or galacton head groups. They dissolve as spherical micelles in boiling water and aggregate to micellar fibers on cooling.[2,3] The octylgluconamide is by far the most soluble in hot water (>50% w/v), followed by the octylmannonamide (2% w/v), and octylgalactonamide (<0.5% w/v).[3] Dodecylamides are in general less soluble by a factor of about ten than octylamides. Octadecylamides are practically insoluble in water and were therefore not included in this study. If one compares the appearance of the fibrous aggregates, then the most soluble gluconamide with a bent head group[3-5] produces the most curved superstructure, namely helical ropes of bimolecular diameters, the mannonamide aggregates to planar bilayer sheets which roll up to scrolls, and galactonamide gives bilayered twisted ribbons.[3] Curvature and twistings are usually lost in nonchiral aggregates. Racemic mixtures of D,L-gluconamides, for example, produce platelets, and D,L-galactonamides appear as smooth tubes (chiral bilayer effect).[4,6]

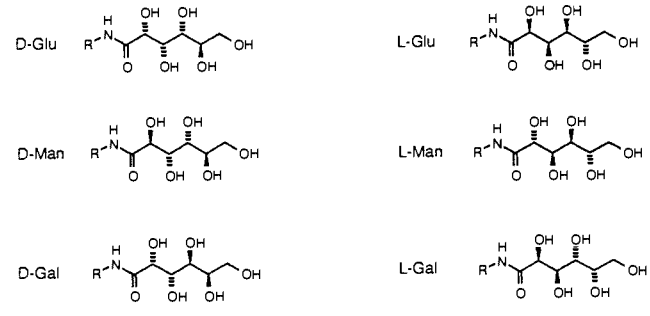

R = $CH_3(CH_2)_7$ = 8

R = $CH_3(CH_2)_{11}$ = 12

Results and Discussion

***N*-Octyl- and Dodecylgluconamides.** A 1:1 mixture of *N*-octyl-D-gluconamide (D-Glu-8) and the dodecyl homologue (D-Glu-12) dissolves in hot water and solidifies to a water-clear gel. Such a gel without any turbidity has so far not been observed for any aqueous gel made from glyconamides. It is a typical example

(1) Nakashima, N.; Asakuma, S.; Kunitake, T. *J. Am. Chem. Soc.* **1985**, *107*, 509-510.
(2) Pfannemüller, B.; Welte, W. *Chem. Phys. Lipids* **1985**, *37*, 227-240.
(3) Fuhrhop, J.-H.; Schnieder, P.; Boekema, E.; Helfrich, W. *J. Am. Chem. Soc.* **1988**, *110*, 2861-2867.
(4) Hortan, D.; Walaszek, Z.; Ekial, I. *Carbohydr. Res.* **1983**, *119*, 263-268.
(5) Fuhrhop, J.-H.; Svenson, S.; Boettcher, C.; Vieth, H.-M.; Rössler, E. Manuscript in preparation.
(6) Fuhrhop, J.-H.; Schnieder, P.; Rosenberg, J.; Boekema, E. *J. Am. Chem. Soc.* **1987**, *109*, 3387-3390.

0002-7863/90/1512-1768$02.50/0

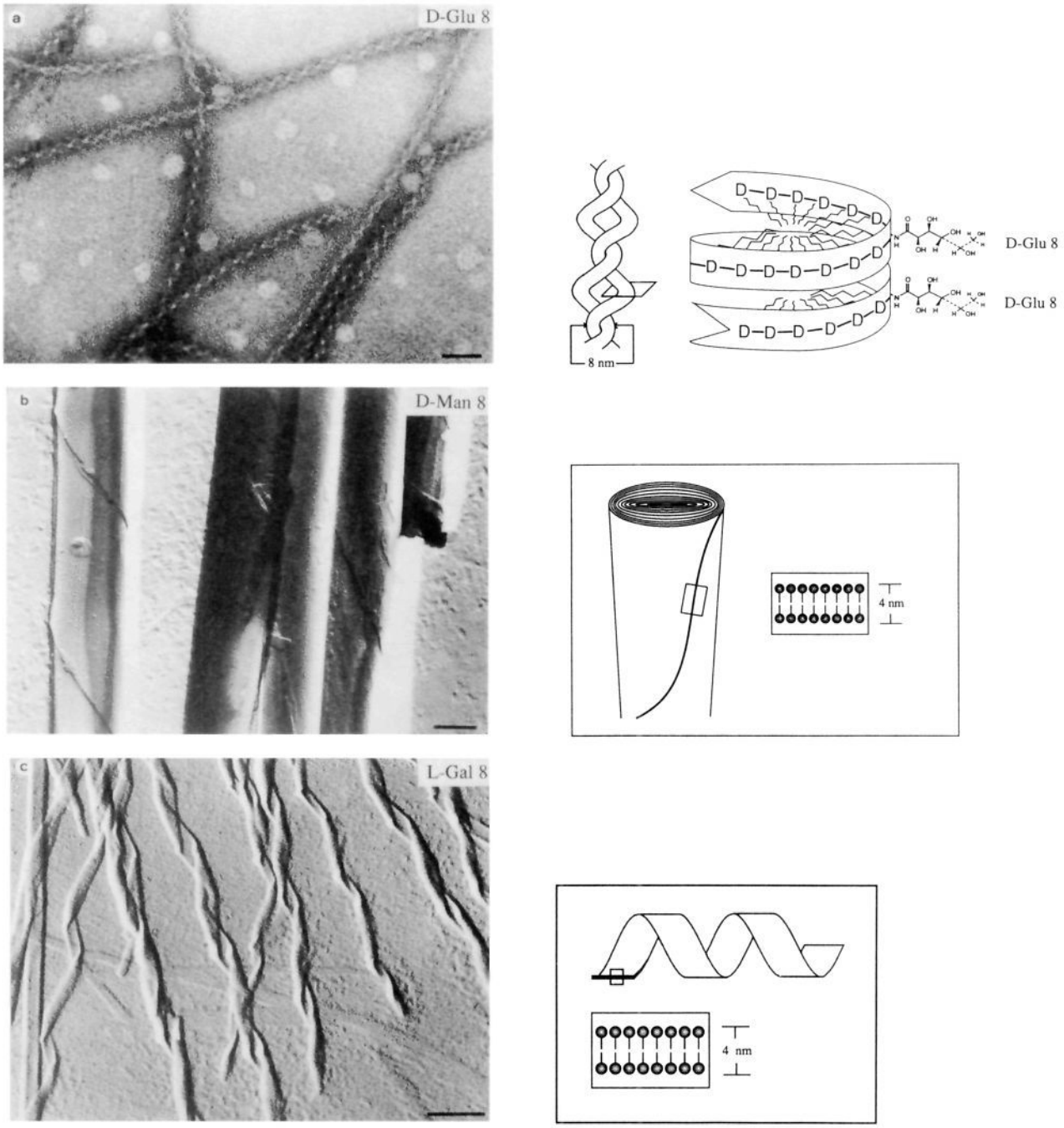

Figure 1. (a) Helical rods from gluconamides (amide hydrogen bonds (–) connect neighboring amphiphile units; bar = 50 nm), (b) rolled up sheets from mannonamides (bar = 300 nm), and (c) twisted ribbons from galactonamides (bar = 300 nm) constitute major types of fibrous lipid bilayers.

for a metastable "alloy". Only organogels from sojalecithin, a complex mixture of double chain amphiphiles, are as clear.[7] Electron micrographs of the clear gel show spherical, large aggregates (diameters 100–1000 nm), which are sometimes connected by helical fibers (Figure 2a, see arrow). Within a minute the clear gel whitens, and the same helical fibers and knot structures are found on electron micrographs, which are known from pure D-Glu-8 or D-Glu-12 gels. The inhomogeneity of chain lengths (i) leads to highly viscous micellar colloids and (ii) retards the formation of well-defined fibers. A surprising finding is that light scattering or turbidity is *not* related to the size of the aggregates. The irregular micellar clusters (Figure 2a) cause much less light scattering as the final gel with thin fibers or, for example, a vesicular solution with 30-nm vesicles. The only rationale, we can offer, is that the particle concentration is relatively low in the clear gel, because much of the amphiphilic material is concentrated within the relatively large spheres. Most of the light, therefore, passes the gel undisturbed and leads to transparency.[8] Rotational disorder of the unequal oligomethylene chains may also contribute to the glass-like appearance. Part of the incident light is, however, diffracted and scattered strongly, which is evident from the orange colorization of objects viewed through the gel. As a primary intermediate stage between the spherical micelles of clear solutions and fibers in the opaque gels, we, therefore, assume droplet-like clusters of spherical micelles. The driving force for this clustering would be the cooperative formation of amide hydrogen bonds, which disturbs the spherical shape of the micelles and thereby exposes part of the hydrophobic chains to the bulk aqueous phase.

(7) Scartazzini, R.; Luisi, P. L. Private communication.

(8) Larsson, K. In *The Lipid Handbook*; Gunstone, F. D., Harwood, I. L., Padley, F. B., Eds.; Chapman and Hall: London, 1986; p 349.

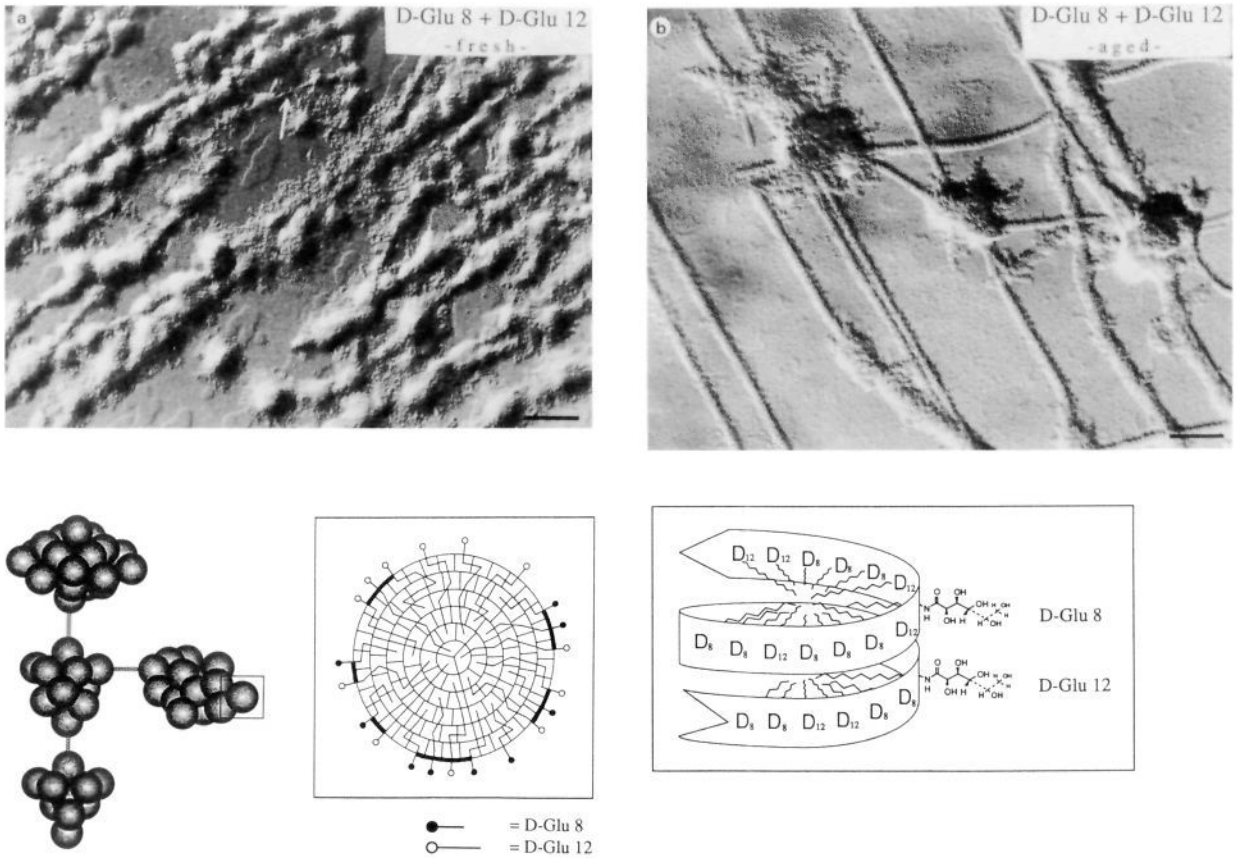

Figure 2. (a) Micellar clusters are often observed in fresh gels (bar = 300 nm) and rearrange (b) to fibers (bar = 200 nm). Smaller clusters may remain as "knots" which now consist of short fibers. The space-filling model cut through a spherical micelle (P. Flory) indicates that only a few headgroups are connected by amide hydrogen bonds (–).

These exposed parts will aggregate randomly, and "oil droplets" are thus formed. The total material contained within these droplets determines the size and number of fibrous aggregate which grow subsequently. No separation of Glu-8 and Glu-12 fibers occurs.

A 2% emulsion of the solid D-Glu-8 and D-Glu-12 (1:1) mixture in water was sealed in a pan for differential scanning calorimetry (DSC) and heated there to 127 °C. The cooling curve showed a relatively weak peak at 61 °C. After reheating the mixture to 127 °C, the second cooling curve showed an even weaker peak at 54 °C. A third cooling curve gave no signal whatsoever. This behavior is in sharp contrast to cooling curves of pure D-Glu-8 and D-Glu-12 gels. Both gave fully reproducible solidification peaks at 78 °C (D-Glu-8) and 97 °C (D-Glu-12), respectively, under identical conditions.[6]

From these results we conclude that the heating to 127 °C of the emulsion did *not* destroy all of the fibers. Presumably some of the D-Glu-12 fibers remained, and cooling restored some D-Glu-8 fibers containing only small amounts of D-Glu-12 as impurity. This caused melting point depression. Later, in the next cooling cycles only ill-defined spherical aggregates of micelles are formed such as shown in Figure 2a. The cooperative formation of amide hydrogen bond chains and fiber formation then takes too long to be observed by DSC. Similar results, namely a drop of solidification points and diminuation of peak areas in consecutive cooling curves, were observed with several other mixtures (see Experimental Section), and the same rationalization applies. We suggest that in all mixtures the first aggregate is just composed of clusters of micelles. Hydrogen bonding of the amide groups will already occur within these clusters, but the formation of defined fibers takes longer time. All the "knots" observed in electron micrographs of aged gels (e.g., Figures 4a,c, 5b, and 6a–c) can be interpreted as remains of such clusters.

If D-Glu-8 is mixed with L-Glu-12, a relatively stable gel is formed, which contains the usual helical fibers. This is in total contrast to the behavior of racemic Glu-8 or Glu-12 alone. In

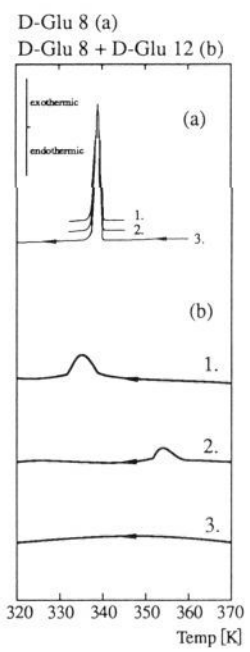

Figure 3. Typical DSC thermograms of mixed glyconamide fiber formation (b) in comparison to uniform glyconamide fibers (a) after repeated registrations (1–3).

these cases platelets instead of fibers are formed.[6] The mixed gel with different chain lengths and different enantiomers as head groups, however, contains P- and M-helices made from D-Glu-8 and L-Glu-12, respectively. This is not only evident from the screw senses of the observed helices but also from differences in the unit's thickness: in the M-helices they are about 1.5 as thick as in the

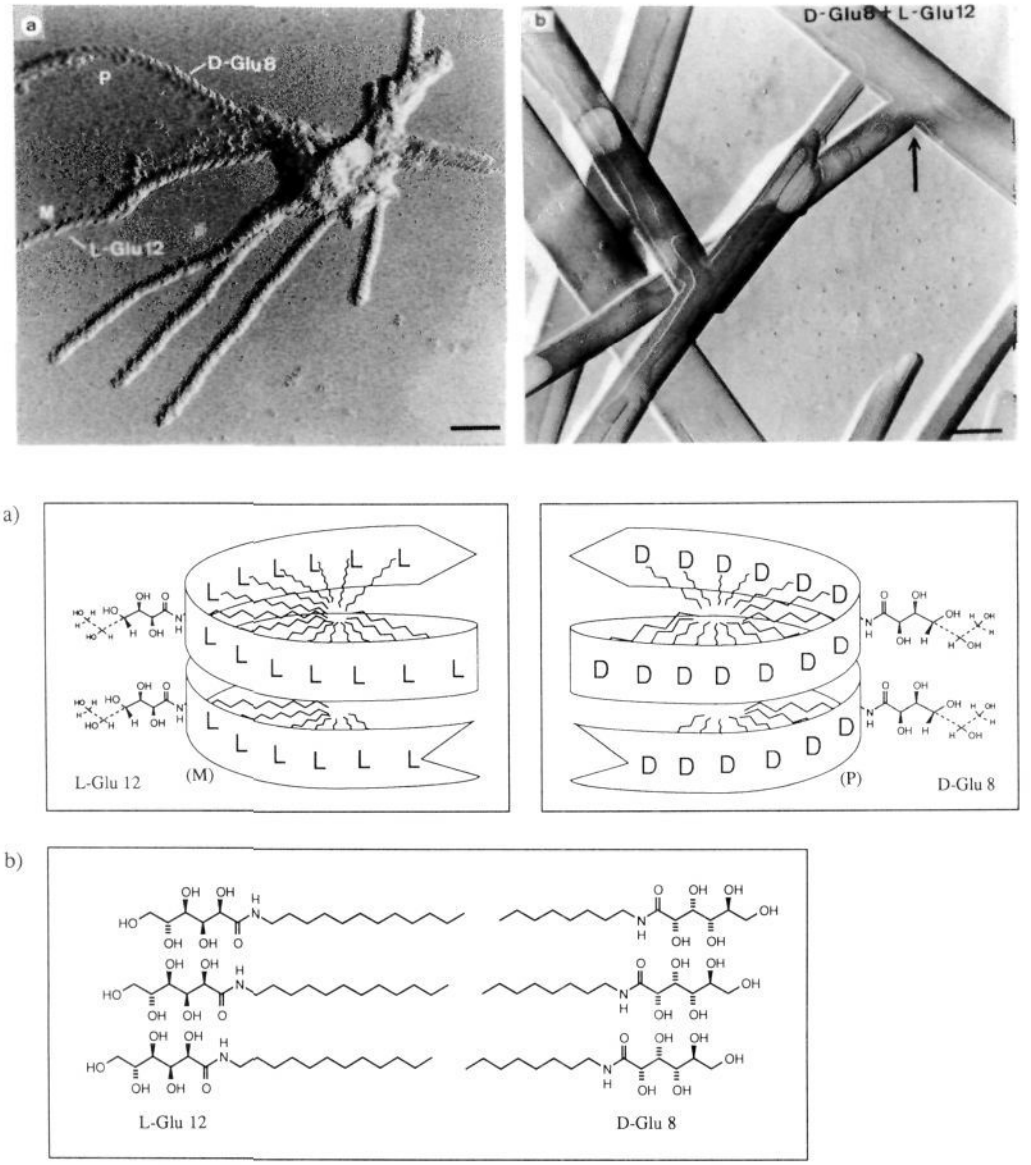

Figure 4. (a,c) P-Helices (D-Glu-8) and M-helices (L-Glu-12) first separate (bar = 100 nm) and then (b,d) unite to form elongated "racemic" platelets (bar = 300 nm). Notice smooth branchings (arrow).

P-helices (Figure 4a). This is in agreement with the facts that L-Glu produces M-helices[6] and bears the longer oligomethylene chain here. One may interpret this observation as "*chain lengths induced racemate resolution*".

These fibers with "enantiomeric" (if one disregards the different chain lengths) fibers are, however, short lived. Almost simultaneously to their growth multilayered, thin crystals appear (Figure 4b,d). We assume that they consist of D-Glu-8–L-Glu-12 bilayers. The measured layer thickness from shadowing was 5 ± 0.5 nm, which agrees with this proposal. Unique features of these crystals, which have never been observed with racemates of uniform chain lengths, are (i) their high length-to-diameter ratio and (ii) their smooth branchings. These observations are explainable with a "retarded chiral bilayer effect". The different chain lengths in both amphiphiles lead to a primary demixing into two different, long fibers A and B, such as shown in Figure 4a,c. These fibers then combine to elongated bilayer piles without curvature. The branching should be favored by the relatively high curvature (Figure 4b,d) of the tips and edges of narrow bilayer platelets. Merging of two such platelets produces perfectly planar bilayers. A sequence of mixed spherical micelles → helical fibers → racemic platelets occurs.

***N*-Octyl- and Dodecylmannonamides.** The stability of the linear all-trans conformation in the mannon head groups favors the formation of planar bilayers.[3] Low solubility of D-Man-12 dictated a 10:1 ratio of D-Man-8:D-Man-12. L-Man-12 was even less soluble in D-Man-8 micelles; a small residue (ca. 10%) of solid *L-Man-12 had always to be removed by filtration from the hot* micellar solution. The analogous observation was made with L-Man-8–D-Man-12 mixtures.

No evidence of separation into different fibers was observed. An analogy to the gluconamide case can be drawn: the D,D-mixture of octyl- and dodecylamides gives the same rolled-up sheets as the single components, whereas the racemic D,L-mixture produces only platelets. Both the enantiomeric head groups and the chains of different lengths do not lead to the fiber separation which was observed as an intermediate state in the case of the C-8 and C-12 D,L-gluconamides. This is caused by the linearity of the mannon head group which leads only to planar, readily miscible bilayers.

***N*-Octyl- and Dodecylamides with Mannon and Glucon Head Groups.** D-Glu-8–D-Man-8 (1:1) mixtures show no tendency to separate. Rapid formation of platelets is observed, and gels are extremely short-lived. D-Glu-8–L-Man-8 (1:1) mixtures, on the other hand, produce separated helical and tubular fibers similar to those obtained from the pure compounds.

We assume that sterical interactions of 1,3-syn hydroxy groups obviously play a much more important role for the curvature of

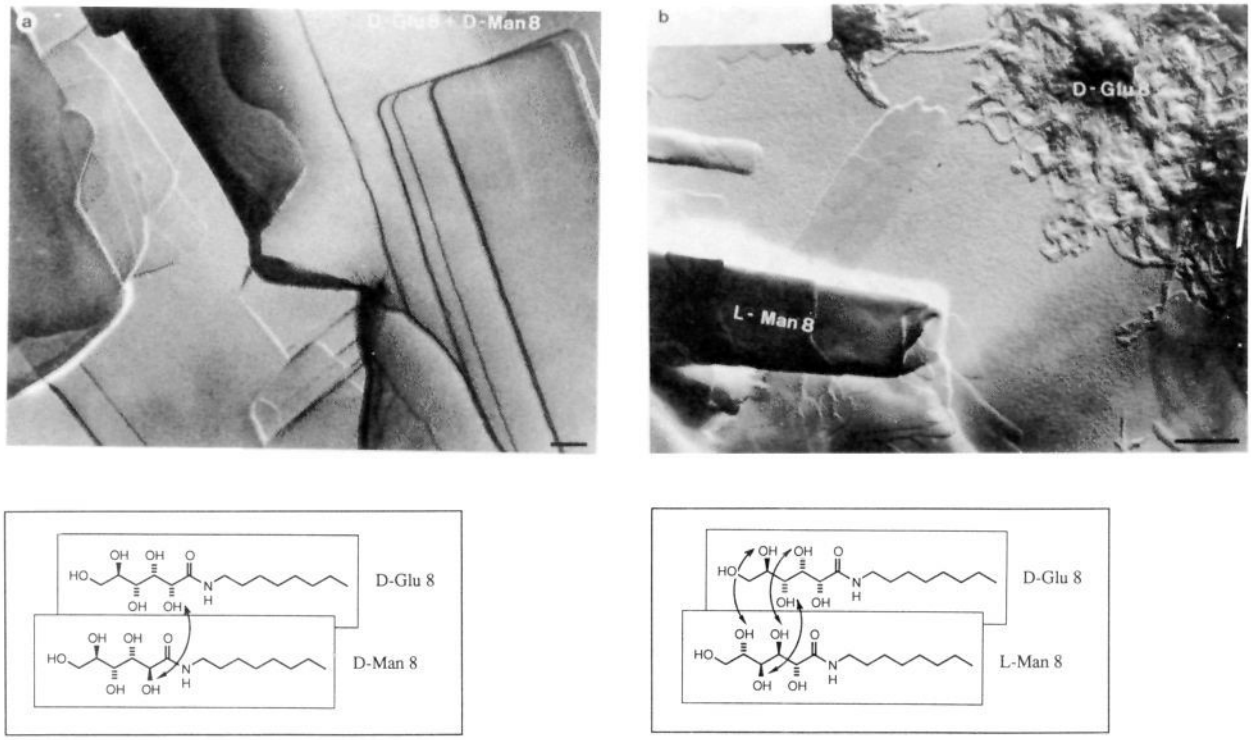

Figure 5. (a) D-Glu-8 is entrapped in D-Man-8 bilayers to form uniform platelets (bar = 100 nm), whereas (b) L-Man-8 does not mix with D-Glu-8 (bar = 300 nm). Separation in (b) is caused by stereochemical differences on the hydrated side of the headgroups.

amphiphilic aggregates if they occur close to the aqueous phase rather than next to the hydrophobic membrane. The amide–hydrogen bond chains presumably overcome the effects of sterical crowding, which then can be further diminished by strong hydrogen bonding between the 1,3-syn positioned hydroxyl groups.[9] Hydroxyl groups on the outer side of the head groups are much more likely to become hydrated. The hydration sphere enhances sterical hindrance and destroys intramolecular bonds. Therefore, D-Man-8 does not separate from D-Glu-8, whereas L-Man-8 does (Figure 5a,b).

Different chain lengths also cause separation in Glu–Man mixtures where the individual aggregates again appear as helical rods and tubes. Demixing of compounds is therefore observed in the case of D-Glu-8–L-Man-12 and D-Glu-8–D-Man-12. The mannonamide tubes are short right after their formation (Figure 6b), and later they grow to the usual size (Figure 6c). The D-Glu-8 helices in the mixed gel are left- *or* right-handed. Such irregularity does not occur with pure D-Glu-8.

In order to explore the purity of the L-Man-12 fibers, D-Glu-8 was tritiated, and the mixed gel was applied to an electron-sensitive micro emulsion. After exposure in the range of 64–120 days the autoradiographs were observed under the electron microscope. Since the mannon aggregates are relatively coarse, they can be clearly distinguished from the fine gluconamide fibers. All of the radioactivity is within the gluconamide fibers, whereas the mannonamide bilayer scrolls contain no radioactive gluconamide. The same holds true for mannonamide platelets which did not roll up (Figure 6a).

An interesting material was obtained from D-Glu-12–D-Man-12 mixtures. Similar to the unresolved D-Glu-8–D-Man-8 platelets no separation whatsoever was observed. The longer chains caused, however, formation of narrow ribbons instead of platelets. The ribbons then rolled up and formed long tubes of extremely uniform diameter (250 nm, "whiskers"), which showed a high tendency to form parallel bundles. We assume that the mannose head group can enforce its linear conformation onto the glucon partner only if the molecular sizes match. Different hydrophobic chain lengths would cause voids in planar bilayers and destabilize them.

D-Glu-12–D-Man-8 and D-Glu-12–L-Man-8 (1:1) mixtures, on the other hand, produce multilayered platelets with curious, ill-defined fringes, presumably made of D-Glu-12, derivable from the uniform srew sense in both cases. This is the only material, where two distinguishable lipid layers remain connected. Low solubility of D-Glu-12 may retard the formation of small micelles needed for material transport. Selective glucon head group hydration then effects a squeeze-out process (see also Figure 11).

Different diastereomers in 1:1 mixtures separate readily (Figures 5b and 6) and usually quantitatively into two different fibers if one of the head groups departs from linearity (glucon), whereas the other is linear (mannon and galacton). Why does then L-Man-8 separate from D-Glu-8, whereas D-Man-8 does not? This is presumably caused by the identity of the three carbon atoms which are exposed to the water surface of D-Glu and D-Man. The rigid mannon head group then enforces a linear conformation onto the glucon moiety, as it is known from gluconamide crystals.[9] In the L-mannon head group, on the other hand, the outer three carbon atoms have a configuration opposite to the configuration of the glucon head group. Crystal-like ordering is not favored any more, and the glucon moiety is free to bend. The same argument applies to D- and L-galactonamide fibers, which both separate from D-gluconamide fibers or D-galactonamide ribbons which separate from L-mannonamides platelets. It is again the difference in the stereochemistry of the hydroxymethine groups close to the water surface that counts.

***N*-Octylgalactonamides Mixtures.** Galactonamides are the least soluble of all glyconamides. Their fibrous aggregates readily separate in the form of tubes or twisted ribons from D-Glu-8 helices. The gels, however, are stable over several months, whereas pure D-Glu-8 or D-Glu-12 gels decompose within a few days to form crystalline precipitates. The twisted ribbons block the formation of enantiomer polar[10] crystals with head-to-tail arrangements in the molecular sheets.[9]

D-Man-8 and L-Gal-8 are differentiated by the configurations at C-3 and C-5. Their 1:1 mixture separates into mannonamide scrolls and galactonamide ribbons (no figure). D-Man-8 and D-Gal-8, on the other hand, are differentiated at the inner carbon atoms C-2 and C-4. Bilayer sheets with rounded corners and edges

(9) Müller-Fahrnow, A.; Hilgenfeld, R.; Hesse, H.; Saenger, W. *Carbohydr. Res.* **1988**, *176*, 165–174.

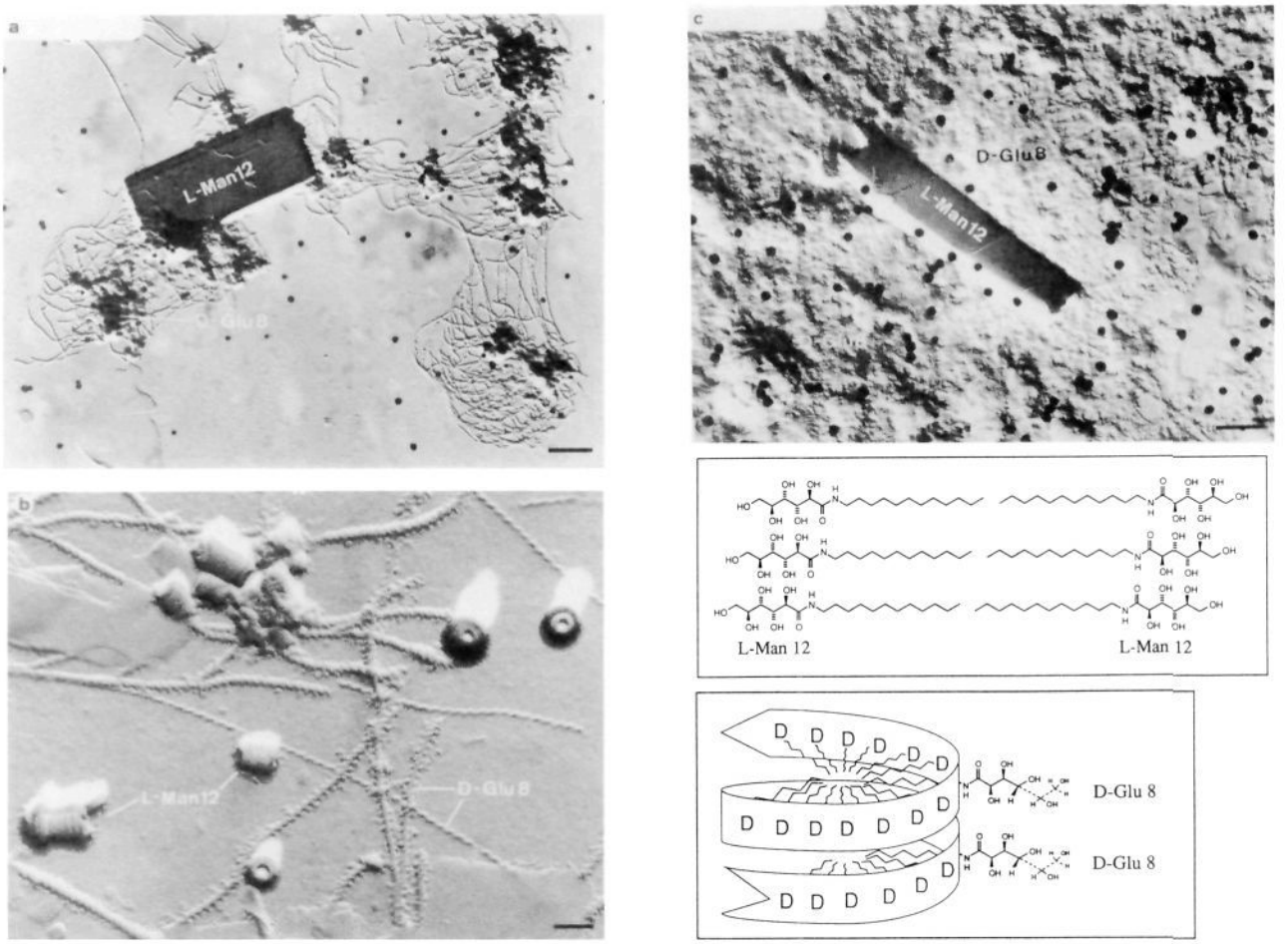

Figure 6. L-Man-12 platelets (a) or tubes (b and c) separate readily from D-Glu-8 helical rods (a, b, and c). In (a and c) D-Glu-8 was tritiated and produces silver grains on autoradiographs (bars: (a) 1 nm, (b) 100 nm, and (c) 500 nm).

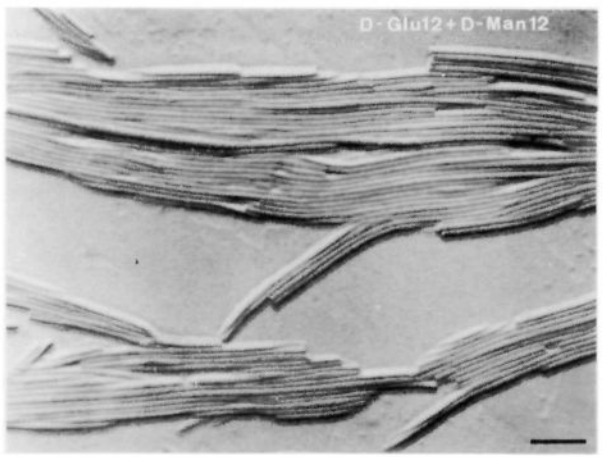

Figure 7. Uniform, whisker-type fibers are formed from dodecylgluconamide–dodecylmannonamide mixtures (bar = 300 nm; compare with the platelets from the octyl analogues in Figure 5a).

are formed exclusively. No trace of the tubes or ribbons formed by the pure compounds is observed (Figure 10). The outer hydroxyl groups obviously again have a more important effect than the hydroxyl groups close to the amide hydrogen bridges (compare with Glu–Man mixtures).

A total of 20 binary mixtures of *N*-octyl- and *N*-dodecylglyconamides with glucon, mannon, and galacton head groups have been examined. All of the 1:1 mixtures gave clear micellar solutions in boiling water, except for those containing Man-8 and Man-12, where only 10% of Man-12 could be dissolved. On cooling to room temperature 14 mixtures solidified to a gel, and

Table I. List of Examined Mixed-Gel Systems and Their Aggregation Behavior[a]

gel system	aggregation behavior[b]	molar ratio	dry weight [mg]	vol [ml]
1. D-Glu-8 + L-Glu-8	P	1:1	25 + 25	5.0
2. D-Glu-12 + L-Glu-12	P	1:1	29 + 29	5.8
3. D-Glu-8 + D-Glu-12	H	1:1	25 + 29	5.4
4. D-Glu-8 + L-Glu-12	S, later P	1:1	25 + 29	5.4
5. D-Man-8 + D-Man-12	H	10:1	25 + 2.9	5.6
6. D-Man-8 + L-Man-12	P	10:1	25 + 2.9	11.2[c]
7. D-Glu-8 + D-Man-8	P	1:1	25 + 25	5.0
8. D-Glu-8 + L-Man-8	S	1:1	25 + 25	5.0
9. D-Glu-8 + D-Man-12	S	1:1	25 + 29	5.4[d]
10. D-Glu-8 + L-Man-12	S	1:1	25 + 29	5.4
11. D-Glu-12 + D-Man-8	B	1:1	29 + 25	5.4
12. D-Glu-12 + L-Man-8	B	1:1	29 + 25	5.4
13. D-Glu-12 + D-Man-12	H	1:1	29 + 29	5.8[e]
14. D-Glu-12 + L-Man-12	P	1:1	29 + 29	5.8
15. D-Glu-8 + D-Gal-8	S	1:1	25 + 25	10.0
16. D-Glu-8 + L-Gal-8	S	1:1	25 + 25	10.0
17. D-Glu-12 + D-Gal-8	S	1:1	29 + 25	10.8
18. D-Glu-12 + L-Gal-8	S	1:1	29 + 25	10.8
19. D-Man-8 + D-Gal-8	P	1:1	25 + 25	10.0
20. D-Man-8 + L-Gal-8	S	1:1	25 + 25	10.0

[a] Solvent is double-distilled water. [b] S = separation, function of individual aggregates for each component; B = heterogeneous mixed structures or "bistructures" (e.g., platelets with fringes); H = homogenous mixed structures, except for platelets; P = mixed bilayer platelets. [c] At lower volumes the material remains insoluble. [d] Clear solution after refluxing. [e] Partly undissolved material.

six gave white precipitates (marked P in Table I). These were the racemic gluconamide mixtures ("chiral bilayer effect", cases 1 and 2) and mixtures containing Man-8 or Man-12 (cases 6, 7,

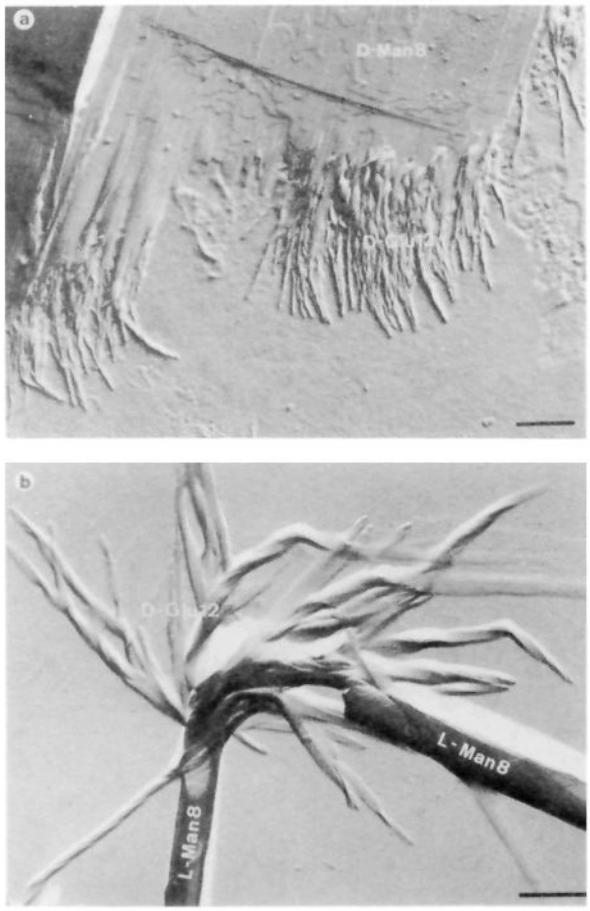

Figure 8. Different chain lengths cause an extrusion process of the glucon component to form heterogeneous structures (compare with the homogeneous structures in Figures 5 and 7; bar = 500 nm).

Figure 9. Gluconamide fibers separate galactonamide ribbons as readily as from mannonamide sheets (see Figure 5b; bar = 200 nm).

14, and 19). Electron micrographs revealed noncurved platelets in all precipitates and fibers in all gels. In the border case of platelets with fibrous fringes (cases 11 and 12) the gels were short-lived, which was also observed with a pseudoracemate containing different chain lengths (case 4).

All gels aged rapidly at room temperature, and precipitates were observed within a day or earlier. The material transport from primarily formed thin aggregates with large surface areas to coarse aggregate structures, and crystals occur by dissociation and reattachment of the micelles. Evidence for such small aggregates comes from ^{1}H NMR spectra of gels, which show some well-resolved signals typical for solutions.[5] Only at elevated temperatures or in the presence of other detergents did the gels remain stable for weeks.

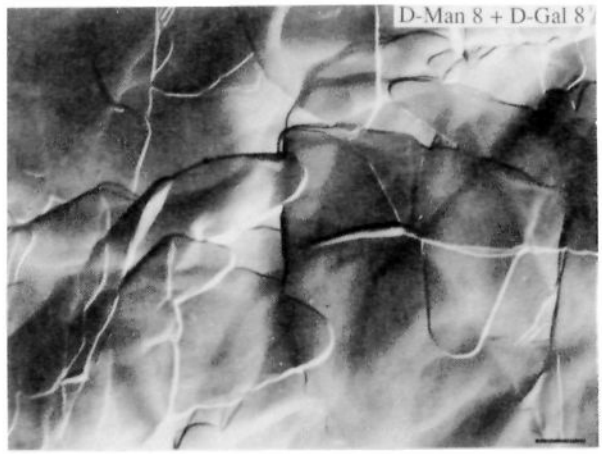

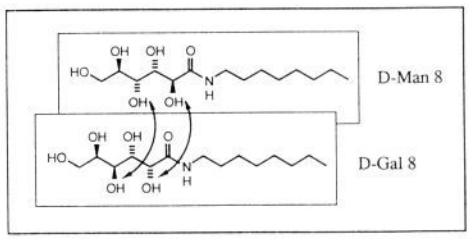

Figure 10. The mannonamide bilayer combines with galactonamide ribbons to homogeneous bilayer platelets (compare with Figure 5; bar = 500 nm).

Three rules of thumbs can be extracted from a comparison of the results given in Table I and the molecular structures of the gluconamides.

(i) Amphiphiles which differ only in chain lengths may lead to water-clear gels containing large spherical aggregates of ill-defined structure (Figure 2a), and no separation occurs. Such structures presumably always occur when small micelles containing different amphiphiles collapse. They are, however, short-lived if the solubility and/or the fiber structures of both components are very different.

(ii) Racemic mixtures crystallize together in the form of square platelets (glucon- and mannonamide) or tubes (galactonamide).[3] The formation of racemic bilayers leads to crystal-like planes, which may roll up. The latter effect is usually only observed with relatively insoluble material.

(iii) Different diastereomers separate readily if the chirality at C-5 and C-3 is opposite.

We conclude that highly curved aggregates made of gluconamides (bent head group) and short alkyl chains (octyl) readily separate from aggregates with less curvature made of galacton- and mannonamide (linear head group) and longer chains (dodecyl). Natural glycolipids usually contain long alkyl chains. We would, therefore, predict homogeneous fibers rather than separation in biological organisates. We also suggest that the axial hydroxyl groups in pyranoid mannose and galactose head groups will have similar curvature-inducing effects as 1,3-syn interactions in open-chain gluconamides. In liquid crystalline phases of lipid–water systems[8] the phase separations between so called hexagonal and lamellar phases, often with intermediate cubic phases, can also be traced back to differences in curvature. The general trends of structural variations with concentrations are as follows: curved structures, namely micelles, their columnar aggregates, and curved patches are favored at relatively low concentration. Structures without curvature, namely bilayered lamellae of infinite extension, are found at higher concentration. Extensive hydration of head groups is obviously the major factor, which causes a relatively large head group diameter and thereby curvature. Less hydrated molecular aggregates are planar. At some water con-

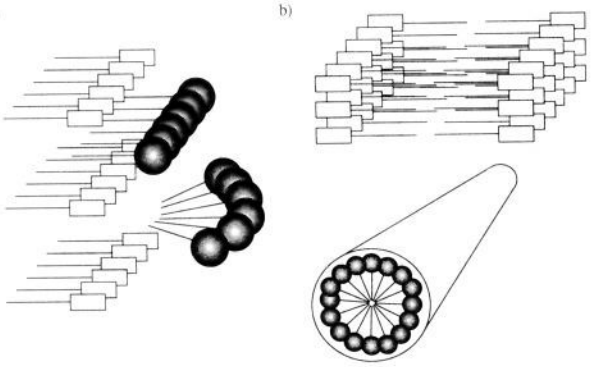

Figure 11. Once a curved bilayer is formed (a), presumably by selective hydration of the head groups, it separates from planar bilayers (b).

centrations hydrated and nonhydrated head groups will coexist, but the different curvature of their aggregates will lead to phase separation.

These conclusions can be loosely correlated to recent theoretical models of chiral lipid aggregates. Shapes of spirals formed by narrow monolayer streaks on water surfaces have been traced back to electrostatic dipolar repulsion and to differences between line tensions on the left- and right-hand sides of the lipid streaks.[11] Another theory employs spontaneous torsion of the bilayer strips to explain helicity and curvature.[12] The twisting of gluconamide rods can indeed be taken as evidence for difference surface tensions at the two opposite faces of the rod. The symmetry of the racemic compounds would remove such differences, and loss of curvature is thus understandable. One may also argue that differences in line tensions are responsible for the separation of fibers. The necessary measurements of bilayer edge torsion and surface tension to check the theories are, however, out of experimental reach for the ultrathin fibers and platelets which are only detectable under the electron microscope. Multilayer tubules and helices[1,20] which are often observable by light microscopy may be more appropriate objects for such measurements, but in these cases the molecular arrangements are usually not known.

The mixed gel systems described in this paper may be useful in molecular machines for the efficient separation of electron donors and acceptors, which are covalently bound to nonmiscible fibers. The "alloys", in particular the whisker-type tubes, may be convertible to polymerized or coated ultrathin tubes. Work along these lines is in progress.

Experimental Section

Synthesis of Hexonamides. The hexonamides D-Glu-8,12, L-Man-8,12, and D,L-Gal-8 were obtained by aminolysis of the corresponding δ-lactones (Sigma) with *n*-octylamine or *n*-dodecylamine in methanol. The γ,δ-lactones, which are suitable for aminolysis leading to the amides L-Glu-8,12 and D-Man-8,12, were prepared by indirect electrolytic oxidation of L-glucose or D-mannose in the presence of calcium bromide and calcium carbonate.[13,14] Excess bromide was precipitated with silver carbonate in the dark. The filtered solution was treated with a strongly acidic ion exchange resin (Merck) and dehydrated by azeotropic distillation with 1-butanol. The same procedure was carried out for the tritium-labeled compound D-Glu-8 by using D-[6-^{3}H]glucose (Amersham) with a specific activity of 5 mCi/mmol and addition of 178.2 mg nonlabeled D-glucose: mp (D,L-Glu-8) = 158 °C, (D,L-Glu-12) = 154 °C, (D,L-Man-8) = 161–162 °C, (D,L-Man-12) = 158–159 °C, (D,L-Gal-8) = 194 °C; $[\alpha]^D_{25}$ (D-Glu-8) = +28.3° (in DMSO), $[\alpha]^D_{25}$ (D-Glu-12) = +22.1° (in DMSO), $[\alpha]^D_{25}$ (D-Man-8) = −18.1° (in DMSO), $[\alpha]^D_{50}$ (D-Man-12) = −17.54° (in DMSO), $[\alpha]^d_{50}$ (D-Gal-8) = +25.5° (in DMSO).

Spectra (IR, ^{1}H NMR, and MS) and elemental analysis (C, H, and N) were in good agreement with expected calculated values.

Table II. Differential Scanning Calorimetry of Glyconamide Mixtures

gel system (see Table I)	repetition[a]	peak characteristics: maximum [°C]	peak characteristics: range [°C]
3. D-Glu-8 + D-Glu-12	1	61	58–64
	2	53	51–55
	3	no signal	
4. D-Glu-8 + L-Glu-12	1	47	43–57
		32	
	2	32	27–37
		22	
	3	20	15–27
	4	no signal	
10. D-Glu-8 + L-Man-12	1	80	72–87
		51	50–52
	2	60	53–67
		40	37–42
	3	44	42–53
		32	31–33
7. D-Glu-8 + D-Man-8	1	64	62–65
8. D-Glu-8 + L-Man-8	1	55	47–57
13. D-Glu-12 + D-Man-12	1	no signal	

[a] Repeated registrations of one sample. Cooling characteristic 2.5 deg/min.

Gels and Micrographs. The gels were formed by heating the described mixtures (Table I) in water to 100 °C and cooling to room temperature. The processes of structure development in the gels were examined by electron microscopy. The specimen were prepared by dipping formvar coated grids (copper, 400 mesh, Balzers) into solution at four different stages: the clear, hot micellar solution, the whitish viscous liquid between 60 and 70 °C, and the fresh and aged gels. The grids were blotted off with the help of a filter paper and dried in air. Platinum/carbon shadowed specimen were made by evaporation under an angle of 35 °C with use of the Edwards coating system E 306 A. For one exception (Figure 1a) the sample was negatively stained by using phosphotungstic acid (2%). Electron microscopy was carried out on a Philips EM 300 at 80 kV, and principle magnifications were between 5000 and 27 000.

All preparations and electron micrographs were repeated at least three times. Only if uniform preparations with many identical objects could be obtained under fully reproducible conditions were the specimen taken up in Table I. It was most critical to start with fully transparent micellar solutions and to take probes at identical temperatures after identical times of cooling. Artefacts, namely ill-defined precipitates, nontypical mixtures, or decorating effects, could be easily detected in series of micrographs.

Autoradiography. Formvar-coated grids (gold, 400 mesh, Balzers) were filmed with a 5.0-nm layer of carbon under an angle of 90°. The preparation followed the analogous conditions of unlabeled material by dipping the grids into the equimolar mixture of *N*-octyl-D-[6-^{3}H]-gluconamide and *N*-dodecyl-L-mannonamide during the formation of the gel. The grids were additionally covered on one side with parafilm to avoid contamination with gel material on both sides. The background was characterized with unlabeled material under identical conditions. The specimen were shadowed with platinum/carbon by evaporation under an angle of 35°. In order to avoid chemography[15] the grids were additionally coated with a 5-nm layer of carbon with an angle of 90°.

Under safelight conditions (no. 902, Ilford) the diluted emulsion (L4, Ilford) was drawn up by using the platinum loop method of Haase and Jung.[16] The thickness of the emulsion layer was determined by interference colors under safelight. The copper-shining part with a film thickness of approximately 1200 Å was used. The exposure occurred in lightproof boxes with silica gel as dehydrant at 4 °C for 64–120 days. Calculations of the radioactive decays yielded an optimum exposure time of about 60 days to obtain ≈1.5 grains per square micrometer. The development followed the method of Lettré and Paweletz.[17] The de-

(10) Addadi, L.; Berkovitch-Yellin, Z.; Weissbuch, I.; van Mil, J.; Shimon, L. J. W.; Lahav, M.; Leiserowitz, L. *Angew. Chem.* **1985**, *97*, 476–496. Enantiomer polar crystals are defined as polar crystals of pure enantiomers. The enantiomers orient uniformly in a crystal plane (p 485).
(11) McConnell, M. H.; Moy, T. V. *J. Phys. Chem.* **1988**, *92*, 4520–4525.
(12) Helfrich, W. *J. Chem. Phys.* **1986**, *85*, 1085–1087.
(13) Frush, H. L.; Isbell, H. I. *Methods Carbohydr. Chem.* **1963**, *2*, 14–18.
(14) Emmerling, W. N.; Pfannemüller, B.; Makromol. *Chem.* **1978**, *179*, 1627–1633.
(15) Salpeter, M. M.; Bachmann, L. In *Principles and Techniques of Electron Microscopy*; Hayat, M. A., Ed.; Van Nostrand Reinhold: New York, 1972; Vol. 2.
(16) Haase, G.; Jung, G. *Naturwissenschaften* **1984**, *51*, 404.
(17) Lettrê, H.; Paweletz, N. *Naturwissenschaften* **1966**, *53*, 263.

veloped grids were dried over night, and electron microscopy was carried out with the Philips EM 300 at 80 kV.

Statistic association of developed silver grains to individual fibers was performed with the X^2-method[18] for evaluation. The X^2-distribution gave significance on a 0.1% level for the following statement: helical fibers are radioactively labeled and contain *N*-octyl-[6-^{3}H]-D-gluconamide. Anisotropic sheets (Figure 6a) and rolled up cylinders (Figure 6c) do not contain labeled material. The emulsion covered with unlabeled materials were developed at the same time as the labeled material. We could not detect any silver grain in this blank preparation. More details on sample preparations and analyses will be given in a technical paper.[19]

Differential Scanning Calorimetry. Seventy μL of the micellar solution of several gel mixtures (Table II) were pipetted into suitable pans. The pans were sealed after formation of the gels at room temperature. DSC was carried out by using the Perkin-Elmer DSC-2C calorimeter. Cooling and heating rates were preset at 2.5 deg/min in the temperature range between 280 and 400 K. The values and peak characteristics are given in Table II.

Acknowledgment. This work was supported by the Sonderforschungsbereich 312 "Vectorial Membrane Processes" of the Deutsche Forschungsgemeinschaft, the Förderungskommission of the Freie Universität Berlin, and the Fonds der Chemischen Industrie.

Registry No. D-Glu-8, 18375-61-6; D-Glu-12, 18375-63-8; D-Man-8, 114275-83-1; D-Man-12, 124915-49-7; D-Gal-8, 114275-82-0; D-Gal-12, 124818-97-9; L-Glu-8, 108032-98-0; L-Glu-12, 124818-98-0; L-Man-8, 114275-90-0; L-Man-12, 124818-99-1; L-Gal-8, 114275-89-7; L-Gal-12, 124819-00-7; D[G-^{3}H]Glu-8, 124779-83-5; 1-octanamine, 111-86-4; 1-dodecanamine, 124-22-1; D-[6-^{3}H]glucose, 3615-68-7; D-glucono-δ-lactone, 90-80-2; L-mannono-δ-lactone, 124915-65-7; D-galactono-δ-lactone, 15892-28-1; L-galactono-δ-lactone, 124819-01-8; L-glucose, 921-60-8; D-mannose, 3458-28-4; L-glucono-γ-lactone, 74464-44-1; D-mannono-γ-lactone, 26301-79-1; D-[6-^{3}H]glucono-γ-lactone, 124755-12-0; L-glucono-δ-lactone, 52153-09-0; D-mannono-δ-lactone, 32746-79-5; D-[6-^{3}H]glucono-δ-lactone, 124755-13-1.

(18) Sachs, L. *Statistische Auswertungsmethoden*; Springer Verlag: Berlin, 1968.
(19) Boettcher, C.; Boekema, E.; Fuhrhop, J.-H. Submitted to *J. Microscopy*.
(20) Schnur, J. M.; Price, R.; Schoen, P.; Yager, P.; Calvert, J. M.; Georger, J.; Singh, A. *Thin Solid Films* **1987**, *152*, 181-206.

In Situ Measurement of the Conductivity of Polypyrrole and Poly[1-methyl-3-(pyrrol-1-ylmethyl)pyridinium]$^+$ as a Function of Potential by Mediated Voltammetry. Redox Conduction or Electronic Conduction?

Huanyu Mao and Peter G. Pickup*

Contribution from the Department of Chemistry, Memorial University of Newfoundland, St. John's, Newfoundland, Canada A1B 3X7. *Received June 26, 1989*

Abstract: The electronic conductivity of polypyrrole and poly[1-methyl-3-(pyrrol-1-ylmethyl)pyridinium]$^+$ (poly-MPMP$^+$) films has been investigated by rotating disk voltammetry. In this in situ measurement, a solution redox species such as cobaltocene, ferrocene, or Cr(2,2′-bipyridine)$_3^+$ serves as an electron source at the polymer/solution interface, while electrons are removed at the polymer/electrode interface. The oxidation state of the polymer is controlled by the potential applied to the electrode. The experimental data have been interpreted in terms of both electronic and redox conduction models. A comparison of the results from these two models reveals that the electronic conductivity and the electron diffusion coefficient are related by the Nernst-Einstein equation. It is concluded that electron transport occurs by a hopping mechanism and that the two models are equivalent descriptions of this process in the pyrrole-based polymers. The electronic conductivity of both polymers initially increases linearly with the degree of oxidation of the polymer backbone (concentration of oxidized sites). The conductivity of polypyrrole rises exponentially from 10^{-8} to 5×10^{-6} Ω^{-1} cm^{-1} over the potential range of −0.7 to −0.4 V, while the electron diffusion coefficient remains constant at ca. 10^{-7} cm^2 s^{-1}. At higher potentials the conductivity is too high to be accurately determined by rotating disk voltammetry. The conductivity of poly-MPMP$^+$ increases from ca. 10^{-9} Ω^{-1} cm^{-1} at +0.35 V to ca. 10^{-4} Ω^{-1} cm^{-1} at +1.0 V.

Conducting polymers are currently receiving much attention because of their many potential applications and their intrinsic scientific interest.[1] Of particular interest is the nature and mechanism of electron transport in these materials, which has been investigated extensively by both theoretical and experimental approaches. Most of the experimental studies have focused on dry polymers, although there have been a number of important in situ studies of the electronic conductivity of polymers immersed in an electrolyte solution. The latter type of study is particularly appropriate to the many electrochemical applications of conducting polymers.

In situ (*solvent-wetted*) conductivity measurements on conducting polymers such as polypyrrole, polythiophene, and polyaniline have been made using microelectrode arrays,[2-4] a twin-electrode thin-layer cell,[5] other twin-electrode arrangements,[6,7] and ac impedance spectroscopy.[8] There have also been numerous in situ studies of electron transport through redox polymers, employing techniques such as chronoamperometry,[9] rotating disk

(1) *Handbook of Conducting Polymers*; Skotheim, T. A., Ed.; Marcel Dekker: New York, 1986.
(2) Kittlesen, G. P.; White, H. S.; Wrighton, M. S. *J. Am. Chem. Soc.* **1984**, *106*, 7389-7396.
(3) Paul, E. W.; Ricco, A. J.; Wrighton, M. S. *J. Phys. Chem.* **1985**, *89*, 1441-1447.
(4) Thackeray, J. W.; White, H. S.; Wrighton, M. S. *J. Phys. Chem.* **1985**, *89*, 5133-5140.
(5) Feldman, B. J.; Burgmayer, P.; Murray, R. W. *J. Am. Chem. Soc.* **1985**, *107*, 872-878.
(6) Gholamian, M.; Suresh Kumar, T. N.; Contractor, A. Q. *Proc. Indian Acad. Sci., Chem. Sci.* **1986**, *97*, 457-464.
(7) Focke, W. W.; Wnek, G. E.; Wei, Y. *J. Phys. Chem.* **1987**, *91*, 5813-5818.
(8) Waller, A. M.; Compton, R. G. *J. Chem. Soc., Faraday Trans. 1* **1989**, *85*, 977-990.

0002-7863/90/1512-1776$02.50/0